Molecular surface chemistry defines nematode development, identity and behaviour

Anna M. Kotowska [1], Fumie Hiramatsu [2], Morgan R. Alexander [1], David J. Scurr [1], James W. Lightfoot [2*], Veeren M. Chauhan [1,3 *]

[1] Advanced Materials and Healthcare Technologies Division, School of Pharmacy, University of Nottingham, University Park Nottingham, NG7 2RD, UK
[2] Max Planck Research Group Genetics of Behavior, Max Planck Institute for Neurobiology of Behavior – caesar, Ludwig-Erhard-Allee 2, 53175, Bonn, Germany.
[3] Lead contact
* Corresponding authors: james.lightfoot@mpinb.mpg.de (JWL), veeren.chauhan@nottingham.ac.uk (VMC)

Abstract: Chemical signalling facilitates organismal communication and coordinates physiological and behavioural processes. In nematodes, chemical signalling has focused on secreted molecules leaving the surface's communicative potential unexplored. Utilising 3D-OrbiSIMS surface-sensitive mass spectrometry, we directly characterise the molecular surface composition of *Caenorhabditis elegans* and *Pristionchus pacificus*. Their surfaces consist of a complex, lipid-dominated landscape with distinct developmental profiles and species-specific characteristics. These surface-anchored chemistries depend on the peroxisomal fatty acid β-oxidation component *daf-22* and are essential for interaction-based behaviours including predation and kin-recognition. Specific lipid molecules identified as putative kin-recognition associated surface components include diglyceride (DG O-50:13), ceramide phosphate (CerP 41:1;O3), and hexosylceramide (HexCer 40:2;O3). Thus, we reveal the nematode surface is a dynamic signalling interface, pivotal for deciphering molecular mechanisms regulating development, identity and contact-dependent behaviour.

Organisms produce a multitude of chemical signals that can be secreted into their surroundings or displayed on their surface (*1, 2*). These signals relay important physiological and environmental information to con-specifics and other co-habitants. However, due to the blend of different chemistries, deciphering the contribution of specific components can be challenging. The nematode *Caenorhabditis elegans*, with its advanced genetic and molecular tools, serves as an important model for understanding chemical signalling (*3*). This has enabled the biological activity and molecular mechanisms involved in the synthesis of a variety of chemical cues to be elucidated. For example, a suite of volatile small molecule pheromones, known as ascarosides, have been found to be secreted into the nematode surroundings and regulate diverse biological processes (*4*). This encompasses regulating development, such as entering the stress-resistant dauer stage, and behaviours, including mate attraction, foraging and aggregation (*5-11*). However, it is likely that these secreted long-range signals are only one facet of the nematode's communication strategy.

The nematode cuticle and its surface coat represent the outermost layer, connecting them with their external environment. In free-living nematodes, the cuticle acts as a permeability barrier (*12*) and must protect these organisms against both external abiotic hazards such as desiccation (*13*), as well as biological factors including pathogenic bacteria (*14*), fungal traps (*15*) and predatory nematodes (*16*). The cuticle comprises crosslinked collagen patterns (*17*), glycoproteins, cuticulins, and lipids (*18*), synthesised by hypodermal cells (*19*). Furthermore, as the nematodes undergo larval moults, their surface coat is replenished and replaced. The expression of many of these components are tightly regulated and oscillate in synchronicity with the organism's development and moult cycle (*20*). Therefore, this sophisticated surface architecture underpins not only the mechanical properties of these organisms, but also its chemical landscape, which plays a crucial role in behaviours, such as locomotion and mating interactions (*21, 22*). Despite the identification of several surface proteins (*23*), the exact chemical composition and the broader significance of the nematode surface as a communication medium remain largely uncharted. This knowledge gap arises not from an absence of curiosity, but from the limitations in available tools for accurately capturing, analysing, and interpreting molecular surface chemistry.

Development influences surface lipids

The study of nematode surfaces has traditionally relied upon methods such as liquid chromatography-mass spectrometry (LC-MS) for analysing homogenates and surface extractions (*24*). Time-of-flight (TOF) based mass spectrometry techniques like Matrix-Assisted Laser Desorption/Ionization (MALDI) (*25*) and Secondary Ion Mass Spectrometry (SIMS) (*26, 27*) have also been used to directly analyse surfaces, although these provide relatively lower mass accuracy. Advancements in surface-sensitive mass spectrometry, such as the 3D-OrbiSIMS, which combines a Gas Cluster Ion Beam (GCIB, Ar3000+) with an Orbitrap analyser (*28*), provide a significant uplift in the ability to understand the chemical complexity of biological samples (*29, 30*), enabling direct surface chemical mapping with relatively high spatial resolution (≥ 2 µm) and mass resolving power (>240,000 at *m/z* 200), achieved in the absence of chemical fixation or additional labelling. Additionally, its field of view (500 µm × 500 µm), facilitates the imaging of the entire length of the nematode, enabling a comprehensive analysis of the organism's chemical composition (**Fig. 1a**). Using this technique, the focus was to investigate the composition of the *C. elegans* surfaces, which consists of rich topological features that generate the organism's external morphology (**Fig. 1b**). Through control of the ion dose (3.00×10^{14} ions/cm^2), the surface analysis was confined to the outermost regions (approximately 50 nm in depth (*31*)), corresponding to the cortical cuticle of *C. elegans* (*18*). Global analysis of adult and newly hatched L1 larvae mass spectra suggested that their surfaces are very similar (**Fig. 1c, fig. S1**). Distribution of molecular assignments into chemical classes (**table S1**), revealed the OrbiSIMS spectra for both the adult and larvae *C. elegans* cuticle coats were dominated by surface-anchored lipids. Specifically, fatty acids and triglycerides (adult 48 % and larvae 43 %) along with

phospholipids (adult 24 % and larvae 29 %) were the major components. Collectively, these components contribute to 72.2 ± 0.6 % of the OrbiSIMS spectra for adults and larvae (**Fig. 1d**). Despite their similar overall chemical profiles, specific chemistries varied significantly between developmental stages. Principal Component Analysis (PCA, **Fig. 1e, fig. S2**) and a hierarchical clustering heatmap (**Fig. 1f**) delineated the developmental stages of *C. elegans* and also initiated the categorisation of distinct chemical profiles responsible for the observed differences in surface chemistry.

Secondary ions exhibiting significant intensity differences across developmental stages (*P<0.001*, Student's t-test) were evaluated using the LIPID Metabolites And Pathways Strategy (LIPID MAPS) database (*32*). This facilitated the identification of molecular species (**Fig. 1g**) and putative structural assignments (**Fig. 1h**) with a mass accuracy of < 2 ppm. Overall, there was a notable increase in the complexity of surface chemistries in adults, characterised by the prevalence of longer-chain fatty acids and triglycerides, which were seldom detectable in larvae. While certain fatty acids, such as FA 20:0, 22:0, and 24:0, were identified in both developmental stages, their intensities remained significantly higher on the surface of adults. Representative normalised intensity maps visually highlight the differences in surface chemistry between *C. elegans* adults and larvae, with FA 20:0 displaying the most pronounced relative intensity across the two developmental stages (**Fig. 1i**). These observations underscore the dynamic and regulated nature of surface composition, reflecting its critical role in the nematode's developmental transitions and adaptation to environmental challenges.

Surface chemistries are *daf-22* dependent

As surface-anchored lipids were prominent on the *C. elegans* cuticle surface, we explored the role of metabolic pathways in producing these chemistries, focusing on the peroxisomal β-oxidation pathway. This pathway is essential for the degradation of very long-chain fatty acids and the synthesis of ascarosides (*33, 34*), with the thiolase DAF-22 acting as the terminal enzyme. *daf-22* mutants show altered fatty acid saturation levels (*35*) and affect ascaroside formation, highlighting its importance for lipid chemistry. We examined *daf-22* mutants in *C. elegans* to assess their impact on surface chemistries across both adult and larval stages (**Fig. 2a**). 3D-OrbiSIMS analysis revealed that *daf-22* mutants lacked several surface chemistries present in both wildtype adults and larvae (**Fig. 1c**). PCA effectively differentiated between the wild type and *daf-22* mutants, which is consistent with substantial alterations to the surface chemistries in *daf-22* animals (**Fig. 2b&c, fig. S3**). In order to identify the precise effects of the *daf-22* mutations on the *C. elegans* surface composition, chemistries were isolated that were exclusive to either adult *C. elegans* wildtype or *daf-22* mutants (**Fig. 2d**). Adult *daf-22* mutants exhibited an absence of higher mass complex surface chemistries (*m/z* 850-950), putatively identified as unsaturated triglycerides (e.g., TG 53:4;O2 and TG 53:6;O3, **Fig. 2e&f**), as well as a reduction in the relative abundance of lower mass ions *m/z* <400 consisting of unsaturated sterols and fatty acids. Instead, an accumulation of mass ions between *m/z* 550–650 were found, putatively identified as diglycerides (*e.g.,* DG O-30:1;O2) and ceramides (*e.g.,* Cer 40:1;O3), as well as unsaturated lysophosphopholipids (**fig. S4**). The larval OrbiSIMS surface composition of *C. elegans daf-22* mutants also differed in a substantial number of chemistries when compared to wildtype at all *m/z* ratios (**Fig. 2g**). In particular, there was an absence of ceramide phosphates between *m/z* 700-800, lysophosphopholipids between *m/z* 400-500 (**Fig. 2h&i**), and cholesteryl ester and unsaturated fatty acids between *m/z* 200-350 (**fig. S4**). Therefore, the peroxisomal β-oxidation pathway is essential for the synthesis of surface-anchored lipids and for establishing the stage-specific surface profile associated with *C. elegans* development.

Evolutionary developmental differences

While *C. elegans* is predominantly found in rotting fruit and is the most well-studied nematode species (*36*), the phylum Nematoda boasts a wide diversity, and encompasses species that have

adapted to a variety of ecological niches. For instance, *Pristionchus pacificus*, a nematode distantly related to *C. elegans*, frequently associates with scarab beetles (*37*). Importantly, the surface properties of nematodes, being in direct contact with their environment, are likely to reflect evolutionary adaptations essential for thriving in specific habitats. For example, *P. pacificus* displays a unique topological surface arrangement (**Fig. 3a**), when compared to *C. elegans* (**Fig. 1b**).Therefore, we conducted direct surface analysis of *P. pacificus* using 3D-OrbiSIMS to explore potential species-specific chemical signatures.

The OrbiSIMS spectra for both *P. pacificus* adults and larvae were again dominated by surface-anchored lipids (**Fig. 3b, fig. S5**). Fatty acids and triglycerides (adult 49 % and larvae 47 %) and phospholipids (adult 24 % and larvae 16 %), contributed to 74 % of the adults and 63 % larvae surface chemistry (**Fig. 3c**). Phospholipid composition variations between *P. pacificus* and *C. elegans* indicate species-specific lipid adaptations. Both PCA (**Fig. 3d, fig. S6**) and hierarchical clustering (**Fig. 3e**) effectively differentiated the developmental stages of *P. pacificus*, revealing a reduction in the number of distinct mass ions characterising *P. pacificus* larvae compared to those observed in *C. elegans*.

Molecular assignments (**Fig. 3f**) and putative chemical structures (**Fig. 3g**) reveal *P. pacificus* adults possess significantly more complex surface chemistries than larvae. The predominant constituents are diglycerides (*e.g.,* DG O-50:13), sterols (*e.g.,* ST 20:0;O2), and a mix of unsaturated (*e.g.,* FA 12:2) and saturated fatty acids (FA 20:0, FA 22:0, and FA 24:0). Representative normalised intensity maps of DG O-50:13, showcasing the most pronounced relative intensity difference, emphasise the observed variations in surface chemistry between *P. pacificus* adults and larvae, further delineating the developmental distinctions (**Fig. 3h**). These observations reinforce previous findings that suggests that the nematode surface profiles are developmentally dependent (**Fig. 3f-h**).

Surface chemistries are species-specific

C. elegans and *P. pacificus* surface chemistry were found to be species-specific and developmentally distinct using PCA analysis (**fig. S7**). By isolating exclusive chemistries from their surfaces for comparative analysis, we discovered a unique cluster of secondary ions in *C. elegans*, ranging from m/z 850-900 (**Fig. 4a**), putatively identified as triglycerides (e.g., TG 48:0;O3, TG 49:2;O3, and TG 49:1;O3, **Fig. 4b**). Whereas *P. pacificus* adults present secondary ions identified as ceramide phosphates (e.g., CerP 46:4;O2) and phosphoethanolamine (e.g., CerPE 51:5;O5) in the higher mass ranges. *C. elegans* larvae surfaces, compared to *P. pacificus* larvae (**Fig. 4c**), were also rich in ceramide phosphosphates (e.g, CerP 43:5,O3, CerP 43:6;O4 and CerP 45:3;O3) as well as a mixture of phosphatidylinositol (e.g., PI 36:5), phosphatidic acids (e.g., PA 38:4) and lysophosphatidic and lysophosphatidylcholine (**Fig. 4d**). *P. pacificus* larvae in general, were absent of surface-specific lipids, compared to *C. elegans* larvae, except for a secondary ion at m/z 782.4788, which was putatively identified as phosphatidylethanolamine (PE 40:10). This analysis highlights species-specific adaptations and shared biochemical pathways across divergent evolutionary paths enhancing our understanding of ecological diversity (**Fig. 4e**). Given the divergent chemistries observed on *C. elegans* and *P. pacificus* surfaces, we also investigated the importance and conservation of the peroxisomal β-oxidation pathway for establishing the surface composition of *P. pacificus* using 3D-OrbiSIMS. Specifically, *P. pacificus* possesses two *daf-22* homologs, *Ppa-daf-22.1* and *Ppa-daf-22.2* (*38*). Analysis of *Ppa-daf-22.1/2* double mutants revealed a reduction in secondary ions and relative intensity (**fig. S8 & S9**), mirroring the findings in observed on *C. elegans* surfaces. Therefore, despite the rapid evolution of the peroxisomal β-oxidation pathway in nematodes, its critical role in establishing the organismal surface profile appears to be conserved between *C. elegans* and *P. pacificus*.

Surface chemistries regulate behaviours

Finally, given the distinct surface chemical profiles observed between *C. elegans* and *P. pacificus*, it was hypothesised that these surface chemistries may function as species-specific communication signals. Nematode mating behaviours are prominently tactile but are strongly impacted by long-distance pheromones, making it challenging to distinguish these effects from contact-specific interactions (*7, 39*). Therefore, to test whether the surface chemistries act as potential communication cues, we directly investigated their role in mediating contact-dependent kin-recognition and killing behaviours in *P. pacificus* using 3D-OrbiSIMS.

P. pacificus use its phenotypically plastic teeth-like denticles to direct predatory behaviour towards other nematode species (**Fig. 5a**) (*16, 40-43*) as well as other *P. pacificus* con-specifics, resulting in highly cannibalistic interactions. However, a kin-recognition system prevents them from killing their direct progeny as well as their close relatives (*44-46*). Crucially, there appears to be little influence from any volatile secreted molecules on this behaviour, which is instead determined by nose contact of the predator with the cuticle surface of a potential prey (*47*). Additionally, a small peptide (*Ppa-self-1*) is known to be essential for the kin signal although the exact mechanism of its action is not yet elucidated (*44*). As mutations in *Ppa-daf-22.1/2* have been shown to result in the acquisition of a distinctive surface chemical profile (**fig. S9**), well-established predation assays (*16, 44*) were used to investigate if this disrupted surface also results in a kin-recognition defect (**Fig. 5b**). Compared to interactions between wild-type animals, which have a robust kin-recognition system to protect their relatives from attack, *P. pacificus* wildtype adults predate on *Ppa-daf-22.1/2* mutant larvae ($P<0.001$). Interestingly, the kin-killing defect observed with *Ppa-daf-22.1/2* mutants was more severe than that observed in *Ppa-self-1* mutants ($P<0.05$). Furthermore, *Ppa-self-1; Ppa-daf-22.1/2* triple mutants demonstrated a stronger synergistic defect than *Ppa-self-1* alone ($P<0.01$, **supplementary movie 1**). Thus *Ppa-daf-22.1/2* is essential for establishing the *P. pacificus* kin-recognition signals.

In order to identify potential chemical surface signals associated with the kin-recognition behaviours the averaged and normalised secondary ion spectra in *Ppa-self-1* larvae were compared to *P. pacificus* wildtype larvae. Distinct surface chemical compositions were identified (**Fig. 5d**), these were further substantiated by PCA analysis (**Fig. 5e, fig. S10**). The analysis identified an absence of secondary ions between *m/z* 775-800 in *Ppa-self-1* mutants (**Fig. 5f**), attributed to the diglyceride DG O-50:13 (M-H, $C_{53}H_{79}O_4^-$, *m/z* 779.5976). This lipid was prominently present in *P. pacificus* wildtype adults and larvae and was also absent in *Ppa-daf-22.1/2* mutants. Additionally, *Ppa-self-1* mutants exhibited an upregulation of mass ions ranging from *m/z* 400 to 750, consisting of diverse chemistries (**Fig. 5g**), including sphingoid base phosphates (e.g., SPBP 17:1;O3), sulphated sterols (e.g., ST 27:4;O;S), simple triglycerides (e.g., TG 30:3), and ceramides (e.g., Cer 39:1;O3, **Fig. 5h**).

Analysis of the *Ppa-self-1; Ppa-daf-22.1/2* triple mutants also reveal distinct surface chemical profiles, evident in the OrbiSIMS spectra (**Fig. 5i**), PCA (**Fig. 5j, fig. S10**), and exclusive mass spectra (**Fig. 5k**). This includes the absence of DG O-50:13 again (**Fig. 5l**) and a range of complex chemistries above *m/z* 550. Simpler chemistries, mainly between *m/z* 350-550 such as saturated fatty acids FA 24:0 and FA 26:0, dominate the remaining profile (**Fig. 5m**). Hierarchical heatmap analysis comparing *P. pacificus* wild-type*, Ppa-self-1*, *Ppa-daf-22.1/2*, and the triple mutant (**Fig. 5n**) reveals distinct, cumulative effect on the chemical signatures. These are characterised by the absence of chemistries in the triple mutants that are downregulated in both *Ppa-self-1* and *Ppa-daf-22.1/2* mutants. In particular, DG O-50:13, along with CerP 41:1;O3, PAO-42:4, and HexCer 40:2;O3, is strikingly absent across all mutated larvae, pointing to their potential role in kin-recognition and predatory behaviours. The high intensity of DG O-50:13 in both adult and larval stages of *P. pacificus* wildtype, contrasted with its absence in mutants suggests it may play a crucial role in establishing the kin-signal and influence behavioural functions. Thus, *self-1* and

Ppa-daf-22 regulate contact dependent behaviours via the establishment of kin-recognition associated surface signals in *P. pacificus* with partial overlapping aspects of their surface profiles.

Discussion

Here, we have performed direct chemical analysis of the outermost 50 nm of the nematode surface using 3D-OrbiSIMS, we have generated an in-depth profile across two developmental stages and two evolutionary distinct species. This represents a significant advance on previous approaches, which utilised homogenate production, surface extraction steps (*24*), or relied on lower-resolution time-of-flight measurements (*26*), significantly refining our comprehension of nematode surface chemistry. We reveal that the nematode surface profile is not a static entity, but instead is comprised of a complex, lipid-dominated landscape, which is dynamically modified during the organism's development. Moreover, the lipid abundance and their hydrophobic properties across both species likely serve as a protective barrier against desiccation, enhancing our understanding of their essential roles beyond simple structural components. The *C. elegans* adult surface is characterised by the prevalence of complex lipid molecules, including longer-chain fatty acids and triglycerides, which are much less common on the larvae. These changes correlate with the maturing nematode metabolism (*48*), resulting in developmental stage specific signals that may be important for distinct population or environmental interactions. Furthermore, by comparing the surface composition across two distinct lineages of free-living nematodes, we also found the surface chemistry is species-specific indicating its importance as an evolutionary adaptive trait. While triglycerides dominate the surface of adult *C. elegans*, the surface of *P. pacificus* is instead comprised of ceramide phosphates, phosphatidylinositol and phosphatidic acids. In addition, the larval surface between species is also strikingly different, with the *P. pacificus* larval surface featuring fewer lipids contributing to its more naïve profile. This may represent a specific adaptation in this species, which could result in a concealed surface that may help avoid detection by predators.

In the predatory *P. pacificus*, distinct chemistries also appear to be associated with transmitting contact mediated information including kin identity. Specifically, in the *P. pacificus* kin-recognition mutants *Ppa-self-1* and *Ppa-daf-22.1/2,* we observed numerous changes in nematode surface chemistry. These findings indicate that kin identity could be transmitted through the synergistic interaction of several surface-anchored components. This is comparable to the cumulative effect observed in many of the small molecule pheromones that regulate the induction of the dauer developmental stage (*7*). Importantly, the surface hydrophobicity and signalling abilities on these nematodes are remarkably similar to those identified in insect species that are surrounded by a waxy layer of cuticular hydrocarbons. These prevent the insect's desiccation but can also communicate information including the sex, age and reproductive status (*49*) as well as nestmate identity as a surrogate for kinship in several social insect species (*50*). Therefore, our studies not only highlight the complexity and dynamism of the nematode surface chemistry, including its plasticity across development and evolution, but also identified a previously undescribed mechanism of communication associated with complex contact-dependent behaviours.

References

1. W. C. Agosta, *Chemical communication: the language of pheromones*. (Henry Holt and Company, 1992).
2. B. W. Ache, J. M. Young, Olfaction: Diverse species, conserved principles. *Neuron* **48**, 417-430 (2005).
3. R. A. Butcher, Decoding chemical communication in nematodes. *Natural Product Reports* **34**, 472-477 (2017).
4. A. H. Ludewig, F. C. Schroeder. (WormBook).
5. P. Y. Jeong *et al.*, Chemical structure and biological activity of the Caenorhabditis elegans dauer-inducing pheromone. *Nature* **433**, 541-545 (2005).
6. R. A. Butcher, M. Fujita, F. C. Schroeder, J. Clardy, Small-molecule pheromones that control dauer development in Caenorhabditis elegans. *Nature Chemical Biology* **3**, 420-422 (2007).
7. J. Srinivasan *et al.*, A blend of small molecules regulates both mating and development in Caenorhabditis elegans. *Nature* **454**, 1115-U1146 (2008).
8. R. A. Butcher, J. R. Ragains, E. Kim, J. Clardy, A potent dauer pheromone component in Caenorhabditis elegans that acts synergistically with other components. *Proceedings of the National Academy of Sciences of the United States of America* **105**, 14288-14292 (2008).
9. E. Z. Macosko *et al.*, A hub-and-spoke circuit drives pheromone attraction and social behaviour in C-elegans. *Nature* **458**, 1171-U1110 (2009).
10. J. Srinivasan *et al.*, A Modular Library of Small Molecule Signals Regulates Social Behaviors in Caenorhabditis elegans. *Plos Biology* **10**, (2012).
11. S. H. von Reuss *et al.*, Comparative Metabolomics Reveals Biogenesis of Ascarosides, a Modular Library of Small-Molecule Signals in C. elegans. *Journal of the American Chemical Society* **134**, 1817-1824 (2012).
12. A. Sandhu, D. Badal, R. Sheokand, S. Tyagi, V. Singh, Specific collagens maintain the cuticle permeability barrier in Caenorhabditis elegans. *Genetics* **217**, (2021).
13. C. Erkut *et al.*, Trehalose Renders the Dauer Larva of Caenorhabditis elegans Resistant to Extreme Desiccation. *Current Biology* **21**, 1331-1336 (2011).
14. C. Couillault, J. J. Ewbank, Diverse bacteria are pathogens of Caenorhabditis elegans. *Infection and Immunity* **70**, 4705-4707 (2002).
15. Y. P. Hsueh, P. Mahanti, F. C. Schroeder, P. W. Sternberg, Nematode-Trapping Fungi Eavesdrop on Nematode Pheromones. *Current Biology* **23**, 83-86 (2013).
16. M. Wilecki, J. W. Lightfoot, V. Susoy, R. J. Sommer, Predatory feeding behaviour in Pristionchus nematodes is dependent on phenotypic plasticity and induced by serotonin. *Journal of Experimental Biology* **218**, 1306-1313 (2015).
17. J. R. G. Adams *et al.*, Nanoscale patterning of collagens in C. elegans apical extracellular matrix. *Nature Communications* **14**, (2023).
18. G. N. Cox, M. Kusch, R. S. Edgar, Cuticle of C*aenorhabditis elegans* - Its Isolation and Partial Characterization *Journal of Cell Biology* **90**, 7-17 (1981).
19. G. N. Cox, M. Kusch, R. S. Edgar, The cuticle of *Caenorhabditis elegans*. II. Stage-specific changes in ultrastructure and protein composition during postembryonic development. *Journal of Cell Biology* **90**, 7-17 (1981).
20. G. J. Hendriks, D. Gaidatzis, F. Aeschimann, H. Grosshans, Extensive Oscillatory Gene Expression during C. elegans Larval Development. *Molecular Cell* **53**, 380-392 (2014).
21. J. Luo, C. Bainbridge, R. M. Miller, A. Barrios, D. S. Portman, *C. elegans* males optimize mate-preference decisions via sex-specific responses to multimodal sensory cues. *Current Biology*, (2023).
22. J. W. Weng *et al.*, Body stiffness is a mechanical property that facilitates contact-mediated mate recognition in Caenorhabditis elegans. *Current Biology* **33**, 3585-+ (2023).

23. M. L. Blaxter, Cuticle surface-proteins of wild-type and mutant *Caenorhabditis elegans*. *Journal of Biological Chemistry* **268**, 6600-6609 (1993).
24. S. Penkov *et al.*, A wax ester promotes collective host finding in the nematode Pristionchus pacificus. *Nature Chemical Biology* **10**, 281-+ (2014).
25. R. F. Menger, C. S. Clendinen, L. A. Searcy, A. S. Edison, R. A. Yost, MALDI Mass Spectrometric Imaging of the Nematode Caenorhabditis elegans. *Current Metabolomics* **3**, 130-137 (2015).
26. F. M. Geier, S. Fearn, J. G. Bundy, D. S. McPhail, ToF-SIMS analysis of biomolecules in the model organism Caenorhabditis elegans. *Surface and Interface Analysis* **45**, 234-236 (2013).
27. V. M. Chauhan *et al.*, The physicochemical fingerprint of *Necator americanus*. *Plos Neglected Tropical Diseases* **11**, 19 (2017).
28. M. K. Passarelli *et al.*, The 3D OrbiSIMS-label-free metabolic imaging with subcellular lateral resolution and high mass-resolving power. *Nature Methods* **14**, 1175-1190 (2017).
29. A. M. Kotowska *et al.*, Protein identification by 3D OrbiSIMS to facilitate in situ imaging and depth profiling. *Nature Communications* **11**, 5832 (2020).
30. N. J. Starr *et al.*, Elucidating the molecular landscape of the stratum corneum. *Proceedings of the National Academy of Sciences* **119**, e2114380119 (2022).
31. J. Bailey *et al.*, 3D ToF-SIMS Imaging of Polymer Multi layer Films Using Argon Cluster Sputter Depth Profiling. *Acs Applied Materials & Interfaces* **7**, 2654-2659 (2015).
32. M. Sud *et al.*, LMSD: LIPID MAPS structure database. *Nucleic Acids Research* **35**, D527-D532 (2007).
33. R. A. Butcher *et al.*, Biosynthesis of the Caenorhabditis elegans dauer pheromone. *Proceedings of the National Academy of Sciences of the United States of America* **106**, 1875-1879 (2009).
34. A. B. Artyukhin *et al.*, Metabolomic "Dark Matter" Dependent on Peroxisomal beta-Oxidation in Caenorhabditis elegans. *Journal of the American Chemical Society* **140**, 2841-2852 (2018).
35. S. B. O. Zhang *et al.*, Genetic and dietary regulation of lipid droplet expansion in Caenorhabditis elegans. *Proceedings of the National Academy of Sciences of the United States of America* **107**, 4640-4645 (2010).
36. M. A. Félix, F. Duveau, Population dynamics and habitat sharing of natural populations of Caenorhabditis elegans and C. briggsae. *Bmc Biology* **10**, (2012).
37. M. Herrmann, W. E. Mayer, R. J. Sommer, Nematodes of the genus Pristionchus are closely associated with scarab beetles and the Colorado potato beetle in Western Europe. *Zoology* **109**, 96-108 (2006).
38. G. V. Markov *et al.*, Functional Conservation and Divergence of daf-22 Paralogs in Pristionchus pacificus Dauer Development. *Molecular Biology and Evolution* **33**, 2506-2514 (2016).
39. Y. Izrayelit *et al.*, Targeted Metabolomics Reveals a Male Pheromone and Sex-Specific Ascaroside Biosynthesis in Caenorhabditis elegans. *Acs Chemical Biology* **7**, 1321-1325 (2012).
40. E. J. Ragsdale, M. R. Müller, C. Rödelsperger, R. J. Sommer, A Developmental Switch Coupled to the Evolution of Plasticity Acts through a Sulfatase. *Cell* **155**, 922-933 (2013).
41. K. T. Quach, S. H. Chalasani, Flexible reprogramming of Pristionchus pacificus motivation for attacking Caenorhabditis elegans in predator-prey competition. *Current Biology* **32**, 1675-+ (2022).
42. W. S. Lo *et al.*, Evolution and Diversity of TGF-β Pathways are Linked with Novel Developmental and Behavioral Traits. *Molecular Biology and Evolution* **39**, (2022).
43. Y. Ishita *et al.*, Co-option of an Astacin Metalloprotease Is Associated with an Evolutionarily Novel Feeding Morphology in a Predatory Nematode. *Molecular Biology and Evolution* **40**, (2023).

44. J. W. Lightfoot *et al.*, Small peptide-mediated self-recognition prevents cannibalism in predatory nematodes. *Science* **364**, 86-+ (2019).
45. J. W. Lightfoot *et al.*, Sex or cannibalism: Polyphenism and kin recognition control social action strategies in nematodes. *Science Advances* **7**, (2021).
46. F. Hiramatsu, J. W. Lightfoot, Kin-recognition and predation shape collective behaviors in the cannibalistic nematode Pristionchus pacificus. *Plos Genetics* **19**, (2023).
47. E. Moreno, J. W. Lightfoot, M. Lenuzzi, R. J. Sommer, Cilia drive developmental plasticity and are essential for efficient prey detection in predatory nematodes. *Proceedings of the Royal Society B-Biological Sciences* **286**, (2019).
48. A. W. Gao *et al.*, A sensitive mass spectrometry platform identifies metabolic changes of life history traits in *C. elegans*. *Scientific Reports* **7**, (2017).
49. G. J. Blomquist, M. D. Ginzel, Chemical Ecology, Biochemistry, and Molecular Biology of Insect Hydrocarbons. *Annual Review of Entomology, Vol 66, 2021* **66**, 45-60 (2021).
50. M. Ozaki *et al.*, Ant nestmate and non-nestmate discrimination by a chemosensory sensillum. *Science* **309**, 311-314 (2005).

Acknowledgments: We would like to thank Monika Scholz and Desiree Götting for discussion and critical reading of the manuscript (MPI Neurobiology of Behavior – caesar, Bonn). Additionally, we wish to thank the Sommer lab (MPI Biology, Tübingen) for providing P. pacificus strains. C. elegans strains were provided by the CGC, which is funded by NIH Office of Research Infrastructure Programs (P40 OD010440).
Funding: This work was funded by a Nottingham Research Fellowship, awarded by the University of Nottingham (VMC). This work was also funded by Max Planck Society (JWL) and by the German Research Foundation (DFG) - project number 495445600 (JWL).
Data availability: All the data are publicly available via the Nottingham Research Data Management Repository at DOI: 10.17639/nott.7386

Author contributions
Conceptualization: VMC, JWL
Methodology: VMC, JWL, FH, AMK
Investigation: VMC, FH, AMK
Visualization: VMC
Funding acquisition: VMC, JWL
Project administration: VMC
Supervision: VMC, JWL
Writing – original draft: VMC, JWL
Writing – review & editing: VMC, JWL, DJS, MRA, FH, AMK

Conflict of interests: The authors declare no competing interests.
Data and materials availability: All the data are publicly available via the Nottingham Research Data Management Repository at DOI: 10.17639/nott.7386
Supplementary Materials
Materials and Methods
Supplementary Method References (51-55)
Supplementary Figures (S1-S10)
Supplementary Table S1
Supplementary Video S1

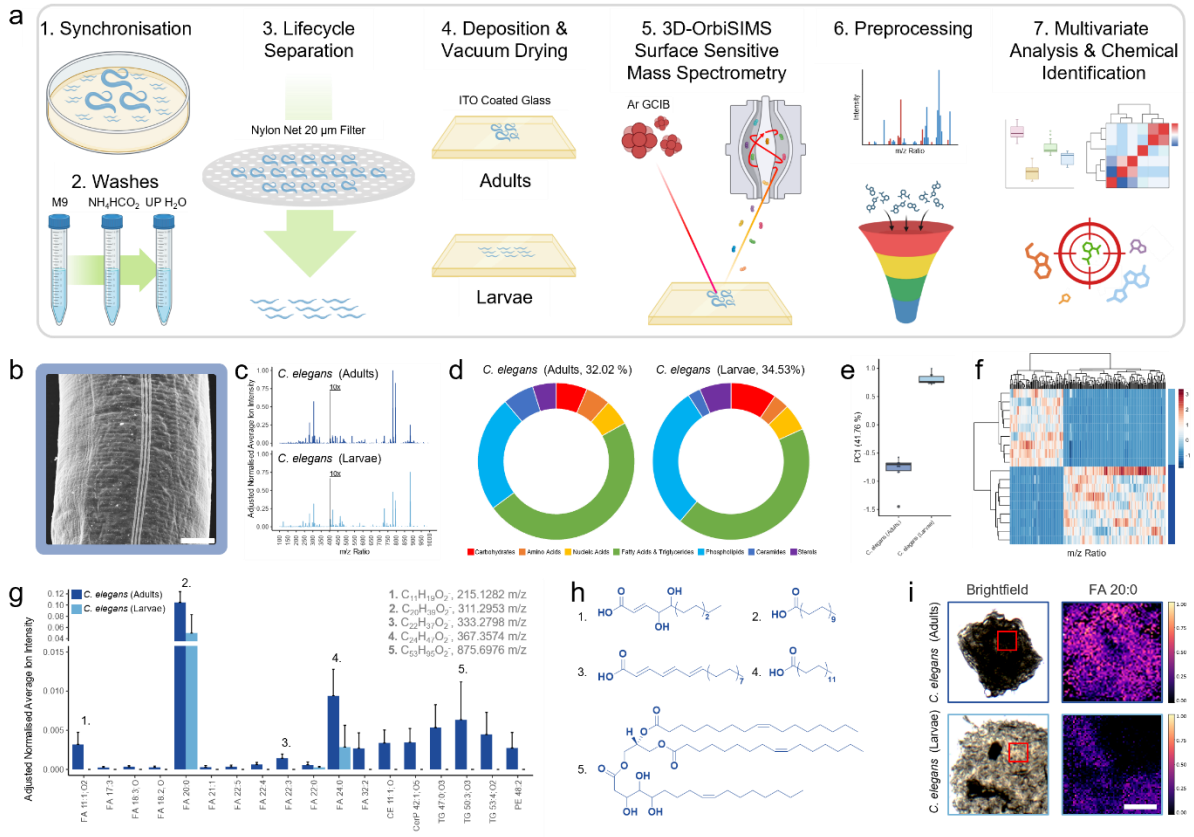

Fig. 1. Surface specific chemistry for *C. elegans* adults and larvae evaluated using 3D-OrbiSIMS. a Schematic detailing capture of adults or larvae surface chemical maps using 3D-OrbiSIMS (100 µm^2, n=9). **b** SEM image of *C. elegans* surface cuticle, scale = 8 µm. **c** Averaged *C. elegans* adults and larvae surface secondary ion mass spectra, normalised to maximum intensity across spectra, where intensity *m/z* >400 enhanced 10x for visibility. **d** Distribution of molecular assignments determined using chemical filtration (**table S1**), as a percentage of total ions surveyed. **e** PCA PC1 scores plot for developmental nematode stages. **f** Hierarchical clustering heatmap for *C. elegans* adults and larvae *m/z* ratio intensity, for PC1 loadings with a standard deviation greater than the mean. Significantly different chemistries on *C. elegans* adults and larvae surfaces (P<0.001 by Student's t-test, n=9) present in LIPIDS MAPS (M-H, <2 ppm) with putative **g** chemical assignments **h** and structures. **i** Representative normalised intensity maps of *C. elegans* adult and larva surface chemistry, scale = 100 µm.

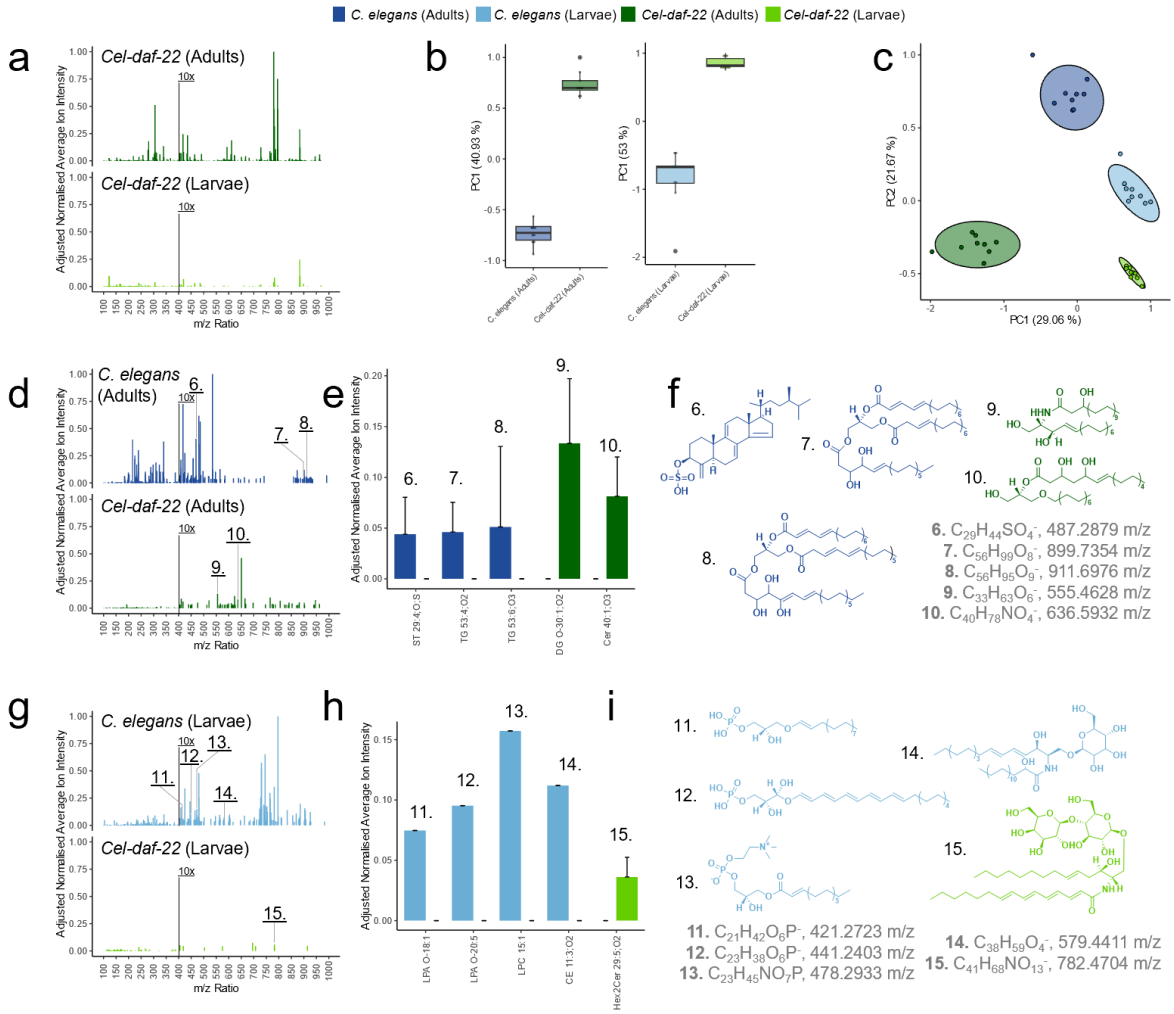

Fig. 2. *C. elegans* surface profile is dependent on *daf-22*. a Averaged *Cel-daf-22* adults and larvae surface secondary ion mass spectra, normalised to maximum intensity across spectra, where intensity *m/z* >400 enhanced 10x for visibility. PCA **b** PC1 and **c** PC1 & PC2 scores plot for *C. elegans* wild type and *Cel-daf-22* developmental nematode stages. Averaged surface secondary ion mass spectra exclusive to *C. elegans* and *Cel-daf-22 (***d** adults and **g** larvae). Putative chemical assignments (**e** adults and **h** larvae) and structures (**f** adults and **i** larvae) on *C. elegans* and *Cel-daf-22* surfaces (*P*<0.001 by Student's t-test, n=9), present in LIPIDS MAPS (M-H, < 2ppm).

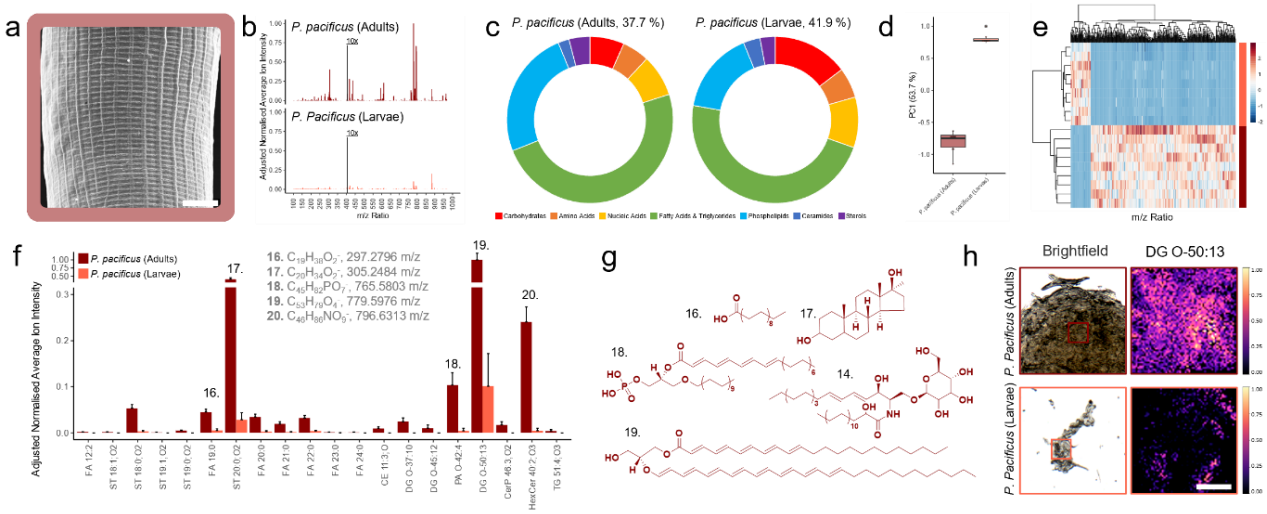

Fig. 3. Surface chemistries are developmental stage dependant. a SEM image of *P. pacificus* surface cuticle, scale = 8 µm. **b** Averaged *P. pacificus* adults and larvae surface secondary ion mass spectra, normalised to maximum intensity across spectra, where intensity *m/z* >400 enhanced 10x for visibility. **c** Distribution of molecular assignments determined using chemical filtration (**table S1**), as a percentage of total ions surveyed. **d** PCA PC1 scores plot for developmental nematode stages. **e** Hierarchical clustering heatmap for *P. pacificus* adults and larvae *m/z* ratio intensity, for PC1 loadings with a standard deviation greater than the mean. Significantly different chemistries on *P. pacificus* adults and larvae surfaces, where (P<0.001 by Student's t-test, n=9), present in LIPIDS MAPS (M-H, < 2 ppm) with putative **f** chemical assignments and **g** structures. **h** Representative normalised intensity maps of *P. pacificus* adults and larvae surface chemistry, scale = 100 µm.

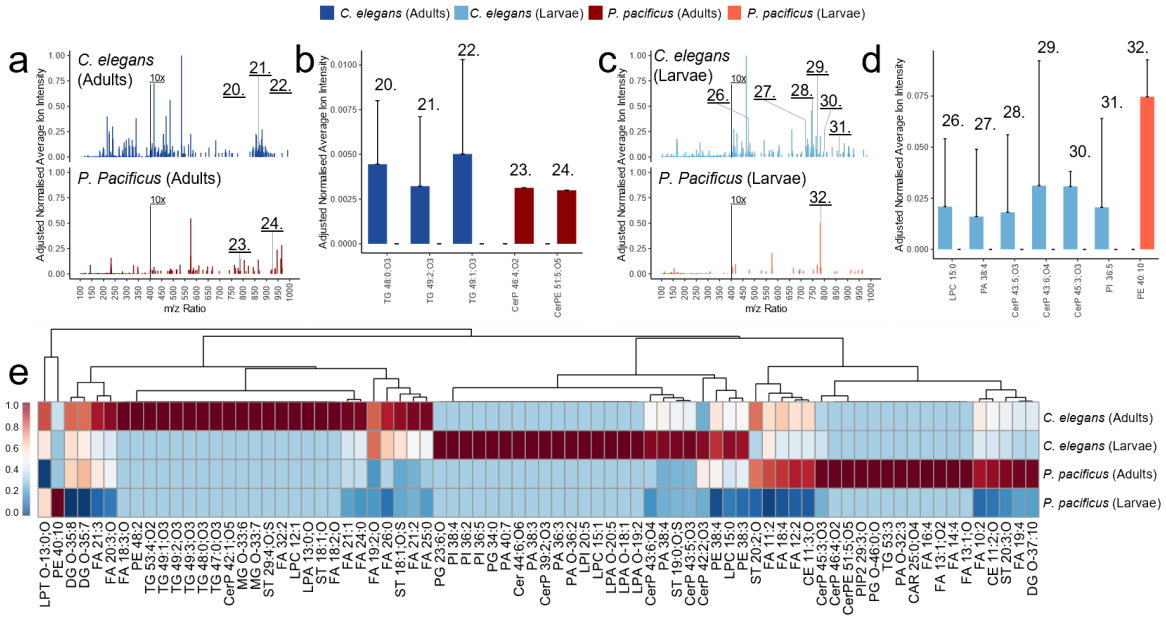

Fig. 4. Surface chemistries are species specific and diverged across evolution. Averaged surface secondary ion mass spectra exclusive to *C. elegans* and *P. pacificus* (**a** adults and **c** larvae). Putative chemical assignments (**b** adults and **d** larvae) on *C. elegans* and *P. pacificus* surfaces (P<0.001 by Student's t-test, n=9), present in LIPIDS MAPS (M-H, < 2ppm). **e** Hierarchical clustering heatmaps of distribution of exclusive chemistries for *C. elegans (*adults & larvae) and *P. pacificus* (adults & larvae), where phylogeny indicates potential shared regulation of exclusive chemicals and their relative intensity on nematode surfaces.

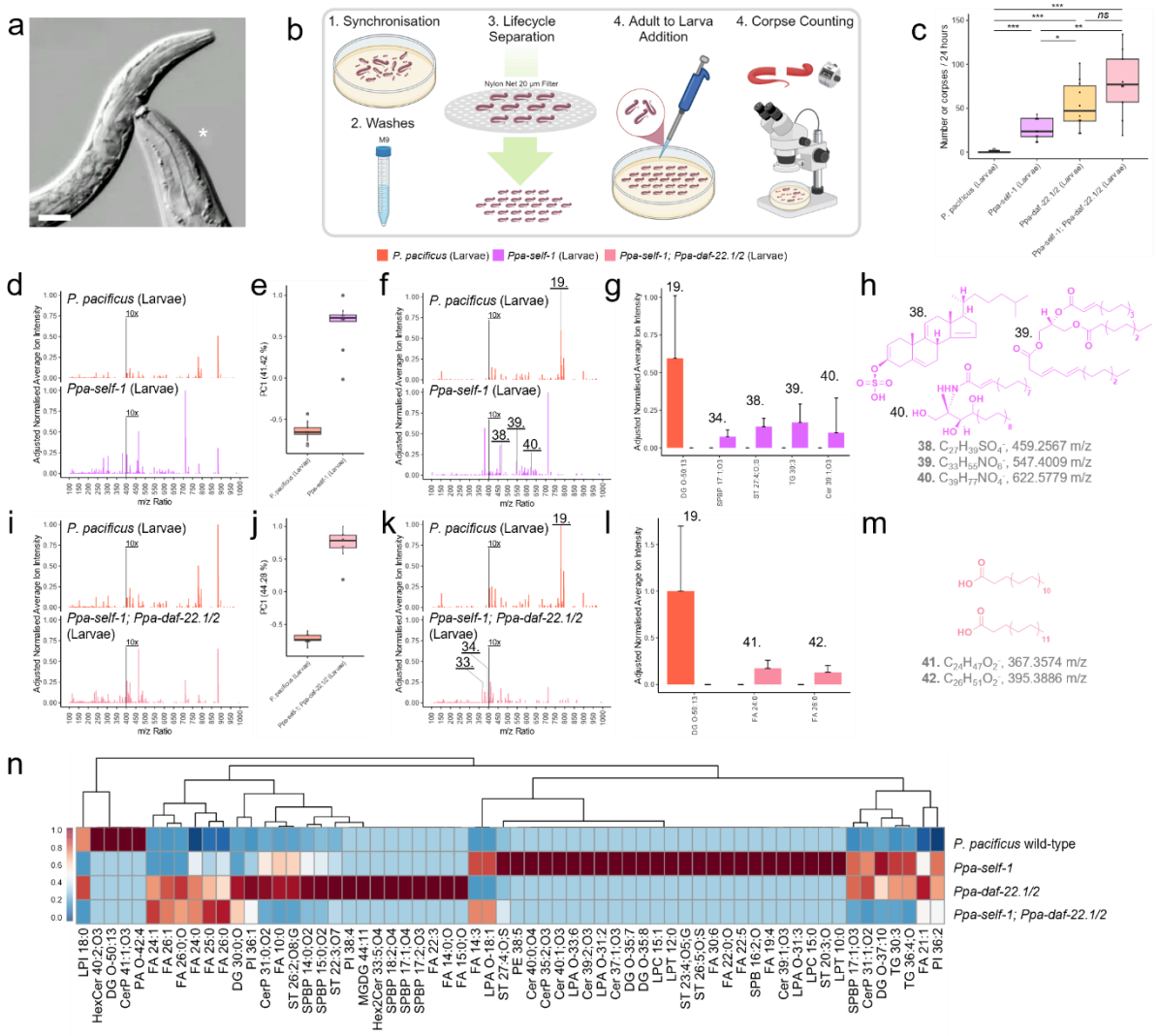

Fig. 5. Surface chemistries regulating contact dependent predatory behaviour. a Representative images of *P. pacificus* wild-type (*) contact dependant predatory biting behaviour towards *C. elegans* wild-type (scale = 20 µm) **b** Schematic of corpse assay of *P. pacificus* preying on kin and mutants. **c** Predatory behaviour of *P. pacificus* wild-type (adult) towards *P. pacificus* wild-type, *Ppa-self-1*, *Ppa-daf-22.1/2* and *Ppa-self-1; Ppa-daf-22.1/2* larvae (ns=*P*>0.05, **P*<0.05, ***P*<0.01,****P*<0.001 - Student's t-test, n=10). Averaged **d** *P. pacificus* larvae & *Ppa-self-1* and **i** *Ppa-self-1; Ppa-daf-22.1/2* and surface secondary ion mass spectra, normalised to maximum intensity across spectra, where intensity *m/z* >400 enhanced 10x for visibility. PCA PC1 scores and plots for **e** *P. pacificus* & *Ppa-self-1* and **j** *P. pacificus & Ppa-self-1; Ppa-daf-22.1/2 larvae*. Averaged surface secondary ion mass spectra exclusive to **f** *P. pacificus* & *Ppa-self-1* and **k** *P. pacificus* & *Ppa-self-1; Ppa-daf-22.1/2*. Putative chemical assignments (**g** and **l**) and (**h** and **m**) structures on for *P. pacificus* & *Ppa-daf-22.1/2* surfaces and *P. pacificus* & *Ppa-self-1; Ppa-daf-22.1/2*, respectively (*P*<0.001 by Student's t-test, n=9), present in LIPIDS MAPS (M-H, < 2ppm). **n** Hierarchical clustering heatmaps of distribution of exclusive chemistries for *P. pacificus* wild-type, *Ppa-self-1*, *Ppa-daf-22.1/2* and *Ppa-self-1; Ppa-daf-22.1/2* larvae, where phylogeny indicates potential shared regulation of exclusive chemicals and their relative intensity on nematode surfaces.